EFFECTS OF ALUMINUM ON THE PRECIPITATION RATE OF SILICA MINERALS

Hanae Saishu[1], Atsushi Okamoto[1] and Noriyoshi Tsuchiya[1]
[1]Graduate School of Environmental Studies, Tohoku University,
6-6-20 Aramaki-aza-aoba, Aoba-ku, Sendai, Miyagi, 980-8579, Japan
e-mail: saishu@geo.kankyo.tohoku.ac.jp

ABSTRACT

The occurrences of silica deposits (quartz veins, silica sinters, silica scales) suggest that precipitation via nucleation and overgrowth on pre-existing mineral surfaces occurs under crustal conditions. We conducted hydrothermal flow-through experiments on silica precipitation using no mineral substrate at 120–430 °C and 31 MPa for understanding the effects of the aluminum on the mineralogy and for deriving rate of the nucleation-controlled precipitation of silica minerals. The dominant silica mineral changes systematically as amorphous silica → cristobalite → quartz with increasing Al concentration, C_{Al}, from 0.0 to 6.7 ppm. The nucleation-controlled precipitation is expressed by a third-order rate equation, and its rate constant depends on C_{Al} and temperature, with an activation energy of 89.6 kJ/mol (C_{Al} = 0 ppm). The overall rate equation for silica precipitation is written as the summation of rates of surface-controlled and nucleation-controlled precipitation. This rate predicts that the dominant precipitation mechanism changes from surface-controlled to nucleation-controlled precipitation with increasing temperature, degree of supersaturation ratio and fracture aperture. This result provides useful constraints on interpretations of the formation of scales in pipelines at geothermal power plants.

Keywords: silica, aluminum, precipitation, kinetics, quartz veins, silica scales

1. INTRODUCTION

Silica precipitation occurs ubiquitously under crustal conditions in various ways, including the formation of quartz veins in the upper and mid crust and the formation of scales at geothermal power plants. The kinetics of dissolution/precipitation of silica minerals affect to temporal and spatial variations in the hydrological and rheological properties of the Earth's crust.

The rate equation of surface-controlled reaction (dissolution and precipitation) of a silica mineral is as follows (Rimstidt and Barnes, 1980):

$$dC_{Si}/dt = k_S (A_i /M) (C_{Si,i,eq} - C_{Si}), \qquad (1)$$

where C_{Si}, $C_{Si,i,eq}$, k_S, A_i, M, and t are the concentration of Si in the solution (ppm), the solubility of silica mineral i, the dissolution or precipitation rate constant, the surface area of silica mineral i, the mass of water in the system, and time, respectively. However, the natural occurrences of various veins suggest that surface-controlled reactions are not always the dominant precipitation mechanism. In addition, minor components in solutions influence the mineralogy and rate of precipitation of silica minerals. Especially, aluminum is one of the main elements in the crust, and is commonly incorporated into quartz and other silica minerals that form under hydrothermal conditions (Miyoshi et al., 2005; Jourdan et al., 2009).

In this study, we conducted hydrothermal flow-through experiments on silica precipitation from solutions with higher Si concentrations. The objective of this study is to (1) clarify the systematic change in the mineralogy of the precipitating silica phase with increasing Al concentration in solution, (2) obtain the rate of nucleation-controlled precipitation of silica minerals, including the effects of temperature and Al concentration in the solution, and (3) obtain the overall rate equation involving the surface-reaction-controlled and nucleation-controlled precipitation of silica minerals. Then we discuss the implications of the dominant precipitation mechanism and the interpretation of the formation of scales in pipelines at geothermal power plants.

2. PREVIOUS WORKS

Some types of quartz veins are interpreted to form as the result of continuous nucleation and growth in fluid (Bons, 2000; Okamoto et al., 2008; Okamoto and Tsuchiya, 2009). Okamoto et al. (2010) showed that both overgrowths on

quartz in the granite and the nucleation of quartz and other silica polymorphs occurred from the solution of Si concentration higher than the solubility of amorphous silica, and that the dominant silica minerals were opal-A (amorphous silica) precipitated from a single-component solution (only Si) and quartz precipitated from a multi-component solution (Si with minor Al, Na, and K).

3. METHODS

The apparatus of hydrothermal flow-through experiments was similar to that used by Okamoto et al. (2010), consisting of three vessels: the R_0 and R_1 were for preparing the input solutions, and the R_2 was for precipitation at 31 ± 1 MPa (Fig. 1). The high-Si solution was prepared by the dissolution of quartz sand in the R_1 vessel at 360 °C. The solution was supersaturated with respect to quartz when it was brought into the R_2 vessel at 430 °C, due to the silica solubility (Fournier and Potter, 1982; Tsuchiya and Hirano, 2007). In the R_2 vessel, we did not set any substrate comprising silica minerals.

To clarify the Al-effect to precipitation of silica minerals, the Al content of the input solution was controlled by the dissolution of albite sand in the R_0 vessel at 160–330 °C. The flow rate was 2.0 ± 0.5 g/min. The concentrations of Si, Al, and Na in the solutions were determined by ICP–AES. The experiment durations were from 76 to 113 hours. The precipitated materials on the tube wall at each segment were identified by XRD.

To obtain the precipitation rate in the absence of a substrate, we assume *n*th-order reactions for the precipitation rate of silica via nucleation, as follows:

$$dC_{Si}/dt = k_P (C_{Si,Qtz,eq} - C_{Si})^n, \quad (2)$$

where k_P is the reaction rate constant of the precipitation of silica minerals in fluids, and n is the reaction rate order. The reaction order of silica precipitation, n, was determined by the integral method. The condition of precipitation experiments was 430 °C, 31 MPa and various residence times, 5.2–31.5 minutes. The input solutions were prepared by the dissolution of silica glass in the R_1 vessel at 360 °C without the addition of minor components, and the R_2 vessel contained no substrate of silica minerals (Fig. 1).

The temperature dependency of k_P was determined from precipitation experiments in the temperature range of 120–430 °C at 31 MPa. The experimental system was the same as that used in the estimates of the reaction order. The flow rate was set to 0.5 ± 0.2 g/min.

4. RESULTS OF EXPERIMENTS

In the experiment of Al-effect, the Si concentration in the input solutions ranged from 268 to 375 ppm, the supersaturation ratio with respect to the solubility of quartz, $\Omega = C_{Si}/C_{Si,Qtz,eq}$, of 2.5–3.8. The Al and Na concentration in input solutions were C_{Al} = 0.0–6.7 ppm and C_{Na} = 0.0–8.2 ppm, respectively. The Si concentration in the output solution essentially decreased from the solubility of amorphous silica (180 ppm), to cristobalite (150 ppm) and then quartz (98 ppm) with increasing of C_{Al}, from < 1 ppm, to C_{Al} = 1–3 ppm and C_{Al} > 3 ppm, respectively. Amorphous silica precipitated dominantly in the experiment with low C_{Al} (Fig. 2a) and quartz was observably dominant in the experiments with high C_{Al} (Fig. 2b). XRD profile of precipitation shows that only amorphous silica precipitated from the solution of C_{Al} = 0.0–0.4 ppm, cristobalite was the dominant crystalline precipitated material in the experiment with C_{Al} = 1.4–3.0 ppm, quartz was observed in the experiments with C_{Al} = 5.6 and 6.7 ppm, and albite precipitated only from the solution of C_{Al} = 6.7 ppm.

In the experiment of the nucleation-controlled precipitation rate, the amount of silica precipitation increased with increasing residence time. The four cases of n = 1–4 were tested for the experimental results. The regression curve was best

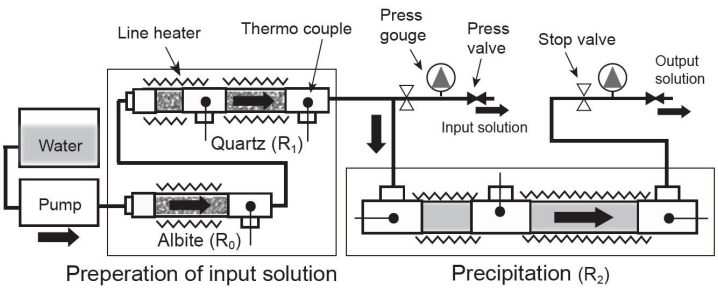

Fig. 1 Schematic illustration showing the basic construction of experimental apparatus for the hydrothermal flow-through

experiment.
fitted in the case of the third-order reaction. The logarithmic values of the precipitation rate constant, log k_P, were calculated by using the third-order rate equation. Log k_P increased linearly from –7.2 to –4.2 ($k_P = 6.3 \times 10^{-8}$ to 5.7×10^{-5} sec^{-1}) with increasing C_{Al} in the input solution from 0.0 to 6.7 ppm. Arrhenius plot for the precipitation rate constant from the solution (C_{Al} = 0 ppm) show high temperature dependency, with activation energy of 89.6 kJ/mol, which was higher than the activation energy of surface-controlled precipitation rate constant, 50.5 kJ/mol, reported by Okamoto et al. (2010). Thus, the dependency of log k_P on temperature, T (K), and C_{Al} (ppm) is written as follows:

$$\log k_P = -0.10 - 4679/T + 0.36 \times C_{Al}. \qquad (3)$$

When silica is precipitated in fractures and pores in crustal rocks, the surface growth of pre-existing quartz surfaces occurs simultaneously with precipitation via nucleation and growth. By combining Eq. 1 (first-order) and Eq. 2 of n = 3 (third-order), the overall rate equation of silica precipitation is empirically expressed as follows:

$$dC_{Si}/dt = k_S (A_{Qtz}/M) (C_{Si,Qtz,eq} - C_{Si}) + k_P (C_{Si,Qtz,eq} - C_{Si})^3. \qquad (4)$$

5. DISCUSSION

Eq.4 includes the relative contributions of surface reactions and nucleation processes to the overall rate of silica precipitation and is useful to consider the texture of precipitation of silica minerals. The boundary between the regions dominated by surface growth and by nucleation was calculated by using Eq.4 and indicates that the dominant precipitation mechanism depends on the supersaturation ratio, the A_{Qtz}/M ratio, temperature, and the Al concentration, because the reaction rate constants are functions of temperature and the Al concentration in solution. In addition, we considered a fracture composed of parallel plates with an aperture w, the A_{Qtz}/M ratio is rewritten by the areal proportion of quartz on the surfaces of the rock fracture, q (in the range from 0 to 1), and the specific volume of water (cm^3/g). The boundary between the surface-reaction-controlled and nucleation-controlled regions always shows a downward concave curve in Ω–T space which calculated under conditions of a geothermal gradient 30 °C/km and q = 0.3. Nucleation-controlled precipitation is dominant at higher temperatures and in regions of higher supersaturation. This trend is consistent with that the energy barrier of nucleation becomes greater at lower temperatures and at lower degrees of supersaturation. The region of surface-reaction-controlled precipitation becomes wider with decreasing fracture width, because of an increase in the A_{Qtz}/M ratio, and the region of nucleation-controlled precipitation becomes wider with increasing Al concentration in solution because of the Al-dependency of k_P (Eq. 3).

The mechanism of silica precipitation (surface-controlled vs. nucleation-controlled) is recorded as the textures of quartz veins. Blocky veins are generally thicker than other types of veins (e.g. elongate-blocky) and indicative of the nucleation-controlled precipitation of quartz. Okamoto et al. (2008) reported that a systematic change in the texture of veins

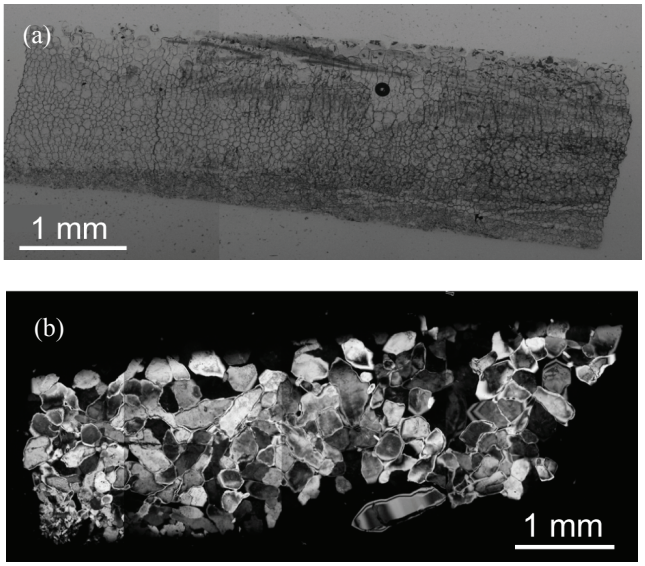

Fig. 2 The optical photomicrograph of products precipitated (a) at 24 cm from the inlet in the experiment with C_{Al} = 1.4

ppm and (b) at 9 cm from the inlet in the experiment with C_{Al} = 6.7 ppm.
is from stretched crystal to elongate-blocky and finally blocky, consistent with the overall rate equations obtained in this study. The supersaturation ratio is higher than 5 in the case of silica precipitating via nucleation processes at 100 °C which is temperature of formation of silica sinters. High Si concentration is possible when fluid ascends from the deep crust, given the low precipitation rate at low temperatures. The formation of silica scales in pipelines of geothermal power plants is consistent with the results of our experiments without rock substrates. The rate equation obtained in this study will be useful in predicting the mineralogy and rate of formation of amorphous silica.

6. SUMMARY

We performed the hydrothermal flow-through experiments and investigated the effect of Al concentration in solution on the mineralogy and rate of nucleation-controlled precipitation of silica minerals as follows:

1. The dominant precipitation of silica minerals from Si-supersaturated solutions change systematically with increasing C_{Al}, in the order of amorphous silica (C_{Al} = 0.0–1.0 ppm), cristobalite (C_{Al} = 1.0–3.0 ppm), and quartz (C_{Al} = 5.0–6.7 ppm).
2. The rate of nucleation-controlled precipitation of silica minerals in fluids is empirically expressed as a third-order rate equation, with a supersaturation ratio defined with respect to quartz. The rate constants, k_p, show a high temperature-dependency, with an activation energy of 89.6 kJ/mol (C_{Al} = 0 ppm), and C_{Al} dependency so that k_p is written as follows: $\log k_p = -0.10 - 4679/T\,(\mathrm{K}) + 0.36 \times C_{Al}\,(\mathrm{ppm})$.
3. The overall rate equation for silica precipitation is obtained as the sum of the contributions of surface growth (first-order reaction) and nucleation + growth (third-order reaction).
4. The dominant mechanism of silica precipitation (surface growth vs. nucleation) in a fracture within crustal rocks depends on temperature, supersaturation ratio, Al concentration in solution, fracture aperture, and the host rock type. Surface growth is predominant under lower temperatures, lower degrees of supersaturation, and in narrower fractures. The precipitation mechanism map is useful for constraining the physico-chemical properties of fluid-filled fractures under crustal conditions.

REFERENCES

Bons P. D. (2000) The formation of veins and their microstructures. *J. Virtual Explorer* **2**.

Fournier R. O. and Potter R. W. II (1982) An equation correlating the solubility of quartz in water from 25 °C to 90 °C up to 10,000 bars. *Geochim. Cosmochim. Acta* **46**, 1969–1979.

Jourdan A. L., Vennemann T. W., Mullis L., Ramseyer K. and Spiers C. J. (2009) Evidence of growth and sector zoning in hydrothermal quartz from Alpine veins. *Eur. J. Mineral.* **21**, 219–231.

Miyoshi N., Yamaguchi Y. and Makino K. (2005) Successive zoning of Al and H in hydrothermal vein quartz. *Am. Mineral.* **90**, 310–315.

Okamoto A. and Tsuchiya N. (2009) Velocity of vertical fluid ascent within vein-forming fractures. *Geology* **37**, 563–566.

Okamoto A., Kikuchi T. and Tsuchiya N. (2008) Mineral distribution within polymineralic veins in the Sanbagawa belt, Japan: implications for mass transfer during vein formation. *Contrib. Mineral. Petrol.* **156**, 323–336.

Okamoto A., Saishu H., Hirano N. and Tsuchiya N. (2010) Mineralogical and textural variation of silica minerals in hydrothermal flow-through experiments: Implications for quartz vein formation. *Geochim. Cosmochim. Acta* **74**, 3692–3706.

Rimstidt J. D. and Barnes H. D. (1980) The kinetics of silica–water reactions. *Geochim. Cosmochim. Acta* **44**, 1683–1699.

Tsuchiya N. and Hirano N. (2007) Chemical reaction diversity of geofluids revealed by hydrothermal experiments under sub- and supercritical states. *Island Arc* **16**, 6–15.